Online Interval Forecast based Operating Reserve Quantification Considering Net-load Uncertainties

Shivani Garg, Arun Kumar Nayak, Rohit Bhakar*, Harpal Tiwari
Department of Electrical Engineering, Malaviya National Institute of Technology, Jaipur, Rajasthan, India
*rbhakar.ee@mnit.ac.in

***Abstract*—The increasing penetration of renewable energy sources (RES) into power grids introduces significant variability and uncertainty in net-load, posing substantial challenges to grid and market operations. Operating reserve, a critical ancillary service, helps in mitigating these challenges. Traditionally, reserve requirements have been quantified using offline learning-based frameworks. However, these frameworks often fail to incorporate recent variations in net-load, limiting their adaptability and responsiveness. This often leads to imbalances in the power system operations, especially during very short-term horizons when rapid net-load variations are most acute. This study proposes a dynamic reserve quantification (RQ) method based on an online interval forecasting approach, addressing these limitations. Additionally, existing studies propose methods for RQ, but they do not address the selection of reserve type and amount in the procurement stage based on individual resource reliability. This study further develops a reliability-aware network constrained market clearing framework to procure reserves from flexible reserve providers. A case study illustrates the proposed method's effectiveness, demonstrating improvements in forecasting accuracy and reductions in reserve procurement costs.**

***Index Terms*—Balancing market, demand response, interval forecast, renewable energy sources, reserve quantification.**

NOMENCLATURE

Sets and Indices

$B, b/\grave{b}$	Set of all buses, indexed by b and $\grave{b}$
E, e	Set of BESS indexed by e
G, g	Set of CGU indexed by g
H, h	Set of PHES indexed by h
L, l	Set for interruptible DR indexed by l
$\grave{L}, \grave{l}$	Set for shiftable DR indexed by $\grave{l}$
S, s	Set of solar units indexed by s
T, t	Set of time intervals indexed by t [15−min]
W, w	Set of wind units indexed by w
ϖ	Market FRP, $\varpi \in \{E, G, H, L, \grave{L}\}$

Variables

$D^{cur}_{b,t}$	Loadshed at time t for bus b [MW]
$P_{\varpi,t}$	Power output of $\varpi \in \{G, L\}$ at time t [MW]
$P^{+/-}_{\varpi,t}$	Scheduled power generation/consumption (discharge/charge) of $\varpi \in \{E, H, \grave{L}\}$ at time t [MW]
$\varrho^{up/dn}_{\varpi,t}$	Up/down regulation allocation of ϖ at t [MW]
$r^{u/d}_{\varpi,t}$	Up/down reserve procured from ϖ at t [MW]
$P^{cur}_{s/w,t}$	Power curtailed from unit s/w at time t [MW]
$\chi_{e,t}$	SOC of e at time t [MWh]

Binary variables

$z_{g,t}$	Running status of g at time t (1-on,0-off)
$u_{g,t}/d_{g,t}$	Start-up/shut-down status variable of g at t
$z^{-/+}_{\varpi,t}$	Charge/discharge (load addition/reduction) status binary variable through $\varpi \in \{E, \grave{L}\}$ at time t
$z_{l,t}$	Binary variable for load reduction for l at time t

Constants and parameters

$C^{(.)}$	Cost of regulation (ϱ) and reserve procured (r) [$/MW]
C_g	Generation cost of CGU g [$]
$C^{su/sd}_g$	Start-up/shut-down cost of unit g [$]
$C^{+/-}_{\varpi}$	Energy production/consumption cost of $\varpi \in \{E, H, \grave{L}\}$ [$/MW]
$C^{rc/lc}$	Penalty for RES/load curtailment [$/MW]
$\sigma^{u/d}_g$	Ramp up/ramp down limit of unit g [MW/15min]
$\kappa^{st/sd}_g$	Start-up/shut-down ramp limit of g [MW/15min]
N_t	Deterministic net-load at time t [MW]
$\bar{P}_{\varpi}/\underline{P}_{\varpi}$	Upper/lower power limits of ϖ [MW]
$\eta^{+/-}_{\varpi}$	Discharging/charging (generation/consumption) efficiency of $\varpi \in \{E, H\}$
$\underline{\chi}_e/\bar{\chi}_e$	Lower/upper SOC limit of BESS e [MWh]
$\bar{R}^{u/d}_t$	Required up/down OR capacity at time t [MW]
Φ_{rel}	Overall required reserve reliability, $\Phi \in [0, 1]$
Φ_{ϖ}	Reliability of FRP $\varpi \in \{E, G, H, L, \grave{L}\}$
$\xi_{b\grave{b}}$	Line limit betweeen buse b and node $\grave{b}$ [MVA]
$\underline{P}^{\varpi}$,$\underline{\Phi}^{\varpi}$	Minimum capacity and reliability requirement of ϖ for FRP participation in market clearing

This work is supported by Department of Science & Technology (DST) TPN-86799 (DST/INT/DAAD/P-19/2023/102).

979-8-3315-1278-1/25/$31.00 ©2025 IEEE

I. INTRODUCTION

THE increasing penetration of renewable energy sources (RES) enhances sustainable energy transition but introduces uncertainty in net-load, the difference between demand and RES generation, impacting real-time grid operations [1]. Operating reserves (OR) are essential for managing these fluctuations, and higher RES penetration increases OR demand to ensure reliability [2]. Given the high costs of reserves, optimizing OR quantification is crucial for economic and efficient grid operation.

Traditional OR quantification approaches often rely on deterministic forecasts (DF), which inadequately capture net-load uncertainties, resulting in over- or under-estimation of reserve requirements, operational inefficiencies, and increased costs [3]. To overcome these limitations, probabilistic forecasting has emerged as an effective method to address the stochastic nature of RES generation. Probabilistic approaches repre-

sent net-load uncertainty through probability density functions (PDF), cumulative distribution functions (CDF), and interval forecasts (IF). PDFs and CDFs are widely applied in stochastic power system optimization, while IF provides a more intuitive representation, estimating the range within which future net-load values are expected to lie with a specified significance level (SL) [4].

IFs can be developed using offline or online learning frameworks. Offline frameworks estimate PDFs of net-load uncertainty to construct intervals based on historical observations, operating in batch mode [5], [6]. However, their inability to adapt to sudden system changes can lead to inaccurate predictions in dynamic scenarios [7]. Online frameworks address this limitation by incorporating continuously updated net-load observations, enabling real-time uncertainty IFs [8]. Online IF frameworks have primarily focused on improving prediction accuracy through statistical metrics [9], [10], often neglecting modern power systems' operational and market requirements. High RES integration introduces variability in OR needs, yet tailored net-load IFs remain under-explored. While online IFs could enhance dynamic balancing markets, practical challenges—such as redefining scheduling, software constraints, and reliance on single models—have hindered their adoption. This work addresses these gaps by integrating IF uncertainty directly into OR quantification, ensuring compatibility with existing scheduling and market-clearing processes.

Furthermore, the existing literature outlines methodologies to help system operators (SO) quantify OR amidst net-load uncertainty. However, these studies overlook the selection of reserve resource type and quantity during procurement based on individual reliability. In the current reserve market, reserves are assumed to deliver 100% reliability, and even Conventional Generating Units (CGU) cannot fully guarantee this reliability due to the risk of forced outages. Additionally, CGUs operate at part-load to provide ORs, which reduces efficiency, potentially increasing fossil fuel consumption and undermining the emission reductions achieved by RES integration [11], [12]. To address these challenges, researchers have proposed using flexible reserve providers (FRPs), such as battery energy storage systems (BESS), pumped-hydro energy storage (PHES), and demand response (DR) techniques, as alternatives for OR provision [13]. However, the existing literature has yet to address reserve procurement based on the individual reliability of these resources, leaving a critical gap in aligning reserve requirements with operational reliability.

FRP can only guarantee a limited percentage of their predicted available capacity due to technical constraints [14]. While FRPs can commit greater capacities to SOs at significantly lower prices, they often avoid participating in the balancing market due to the heavy penalties for non-delivery [15]. A reliability-aware reserve procurement approach can encourage FRPs to supply reserves at competitive prices, enhancing market liquidity and reducing operational costs [12]. However, while few studies address reliability-aware market clearing, none incorporate network constraints [14], [15]. A network-constrained market clearing model that co-optimizes energy and reserves ensures feasible dispatch by considering transmission limits and voltage constraints. This helps in maintaining grid's operational efficiency, unlike unconstrained methods, which may lead to sub-optimal dispatch [16].

In this context, major contributions from this study are two fold:

1) An online ensemble learning-based interval forecast (OELIF) method is developed to address net-load uncertainty.
2) A network-constrained reliability-aware market clearing model is proposed that optimally co-optimizes energy and reserves while incorporating different FRPs viz., BESS, PHES, CGU, interruptible and shiftable DR.

The rest of the paper is organized as follows: the OELIF based net-load uncertainty is modeled in Section II. The reliability aware reserve procurement problem framework is formulated in Section III. Results are discussed in Section IV, followed by the conclusion in Section V.

II. OELIF Uncertainty Model

The online IFs considering net-load as the target variable, uses bootstrap aggregation technique, adapted for real-time data streams. It combines multiple regression models as base learners improving overall prediction accuracy while being able to update with new data in an online fashion.

A. Problem Definition

Given a stream of data arriving sequentially,

$$\Gamma = \{(\mathbf{X}_{(t,j)}, N_t)\}_{t=1}^{\infty} \tag{1}$$

where, $\mathbf{X}t, j \in \mathbb{R}^J$ be the J-dimensional feature vector at time t, and $N_t \in \mathbb{R}$ be the target variable (net-load) at time t. The goal is to develop an online model that predicts the target $\hat{N}t$ using $\mathbf{X}t, j$. An ensemble of linear regression models serves as base learners, updated incrementally with new data. In the ensemble, k represents the number of base learners, and $M_k(\mathbf{X}(t,j);\theta_k)$ denotes the prediction of the k^{th} base learner with parameters θ_k, where $\beta_{k,o}$ is the bias and $\beta_{k,j}$ the coefficient of the j^{th} feature.

$$M_k(\mathbf{X}_{(t,j)};\theta_k) = \beta_{k,o} + \sum_{j=1}^{J} \beta_{k,j}\mathbf{X}_{t,j} \tag{2}$$

Each base learner is trained independently on a distinct data subset, typically obtained via bootstrap sampling. In an online setting, this process is simulated incrementally using subsampling. Unlike traditional batch learning, where multiple bootstrap samples are generated for training, the predictions from all models are averaged to produce the final prediction.

B. Bootstrap Sampling in Online Setting

In the online setting, generating bootstrap samples is not feasible due to sequential data arrival and the impracticality of storing the entire dataset. For each incoming observation $(\mathbf{X}_{(t,j)}, N_t)$, the weight of each base model M_k in the ensemble is computed using the rolling mean of past prediction

errors, such as Mean Squared Error (MSE). The rolling mean error for model M_k is:

$$MSE_k^{(t)} = \frac{1}{w} \sum_{\tau=t-w+1}^{t} \varepsilon_{k,\tau}, \quad for \quad t \geq w \tag{3}$$

Where, $\varepsilon_{k,t} = (N_t - M_k(\mathbf{X}_{(t,j)}; \theta_k))^2$ be the squared error of the model M_k, on the observation $(\mathbf{X}_{(t,j)}, N_t)$.

$$\theta_k^{(t)} = \frac{1}{MSE_k^{(t)} + \iota} \tag{4}$$

Where, $\iota > 0$ is a small constant preventing division by zero. Each base learner M_k is updated using an online learning algorithm (e.g., Online Gradient Descent, Stochastic Gradient Descent) whenever a new observation is included [17].

$$\theta_k^{(t+1)} = \theta_k^{(t)} - \vartheta \nabla_{\theta_k} \mathcal{L}(N_t, M_k(\mathbf{X}_{(t,j)}; \theta_k)) \tag{5}$$

where, ϑ is the learning rate and $\mathcal{L}(N_t, M_k(\mathbf{X}_{(t,j)}; \theta_k))$ is the loss function, typically squared error of the model M_k.

$$\mathcal{L}(N_t, M_k(\mathbf{X}_{(t,j)}; \theta_k)) = \frac{1}{2} \varepsilon_{k,t} \tag{6}$$

C. Point Ensemble Prediction

The final prediction of the online ensemble model $\hat{N}_t$ is computed as the weighted combination of the predictions of K base learners [18].

$$\hat{N}_t = \frac{\sum_{k=1}^{K} \theta_k^{(t)} M_k(\mathbf{X}_{(t,j)}; \theta_k))}{\sum_{k=1}^{K} \theta_k^{(t)}} \tag{7}$$

Algorithm 1 OELIF-Protocol:

- **Input**: Data stream $\Gamma = \{(\mathbf{X}_{(t,j)}, N_t)\}_{t=1}^{\infty}$, Number of models K, Quantile array, $Q = [0.025, ...0.975]$, Loss function, $\mathcal{L}(\theta)$, Learning rate, ϑ, Quantile, q
- **Initialize**: K models $M_1, M_2, \ldots, M_K$
- **For each** data point $(\mathbf{X}_{(t,j)}, N_t)$ in the stream:
  - **For each** model M_k $(k = 1, \ldots, K)$:
    - Obtain $MSE_k^{(t)}, \theta_k^{(t)}$
  - **Ensemble prediction**: Following Equation (7)
  - **Interval Forecasts**: **If** $q \in Q$:
    - Quantile prediction, $\hat{N}_{t,q} = \theta_{\iota,q}^{(t)} \cdot \hat{N}_t$
    - Actual values, $N_t \in \mathbb{R}$;
    - Probabilistic loss function, $\mathcal{L}_q(N_t, \hat{N}_{t,q})$
    - Update model, $\theta_{\iota,q}^{(t+1)} = \vartheta \left(\theta_{\iota,q}^{(t)}; \mathcal{L}_q(N_t, \hat{N}_{t,q})\right)$

    else $\theta_{\iota,q}^{(t)} = \theta_{\iota,q}^{(t+1)}$
- **Output**: Projected Quantiles, θ_q, $\forall\ q \in Q$

D. Online IFs

The IF method of probabilistic forecasting estimates the range of forecast variables within which a future observation is likely to fall. Unlike a confidence interval, which estimates the range for a population parameter, an IF provides the range for a single future observation. The size of the IF depends on the desired SL, inherent data variability, and the sample size. An IF at a time step t at SL α is defined as:

$$\hat{I}_{t|t-1}^{(\alpha)} = \hat{N}_{t|t-1}^{(q=\alpha/2)} - \hat{N}_{t|t-1}^{(q=1-\alpha/2)} \tag{8}$$

Where, $\hat{N}_{t|t-1}^{(q=\alpha/2)}$ and $\hat{N}_{t|t-1}^{(q=1-\alpha/2)}$ are the upper and lower boundaries of the $\hat{I}_{t|t-1}^{(\alpha)}$ respectively [18].

E. Reserve Quantification

In industry practice, OR for net-load uncertainty are based on deviations between actual net-load and dispatched levels. To account for uncertainties, an interval around the net-load point prediction is defined at a specified SL α. The difference between the net-load PI bounds and point prediction defines up and down OR requirement [8].

$$\bar{R}_t^{up} = \hat{N}_{t|t-1}^{(q=\alpha/2)} - N_t, \ \bar{R}_t^{dn} = N_t - \hat{N}_{t|t-1}^{(q=1-\alpha/2)}; \forall t \tag{9}$$

III. Reliability Aware Reserve Procurement

This section presents a reliability aware network-constrained market-clearing model, where anticipated demand and reserves are procured using various FRPs within a mixed-integer linear optimization framework.

A. Objective Function

The scheduling problem seeks to minimize the total cost associated with energy procurement, regulation, reliability-aware reserves, and penalties for load/RES curtailment in the day-ahead market. This is given in (10).

$$Obj = min(\lambda^{ene} + \lambda^{reg} + \lambda^{res} + \lambda^{pen}) \tag{10}$$

The terms $\lambda^{(\cdot)}$ denotes the total cost associated with energy generation (11), regulation (12), reliability aware reserve (13), and penalty for load/renewable curtailment (14).

$$\lambda^{ene} = \sum_{g,t} C_g P_{g,t} z_{g,t} + \sum_{g,t} (C_g^{su} u_{g,t} + C_g^{sd} d_{g,t}) + \sum_{e,t} C_e^- P_{e,t}^- \sum_{h,t} (C_h^+ P_{h,t}^+ + C_h^- P_{h,t}^-) + \sum_{l,t} C_l P_{l,t} + \sum_{\grave{l},t} C_{\grave{l}}^- P_{\grave{l},t}^- \tag{11}$$

$$\lambda^{reg} = C^{\varrho}[\sum_{\varpi_{\varpi \neq l},t} (\varrho_{\varpi,t}^{up} + \varrho_{\varpi,t}^{dn}) + \sum_{l,t} \varrho_{l,t}^{up}] \tag{12}$$

$$\lambda^{res} = C^{r}[\sum_{\varpi_{\varpi \neq l},t} \Phi_{\varpi}(r_{\varpi,t}^{u} + r_{\varpi,t}^{d}) + \sum_{l,t} \Phi_l r_{l,t}^{u}] \tag{13}$$

$$\lambda^{pen} = C^{rc}[\sum_{s,t} P_{s,t}^{cur} + \sum_{w,t} P_{w,t}^{cur}] + C^{lc} \sum_{b,t} D_{b,t}^{cur} \tag{14}$$

The first term in (11) represents the linearized quadratic cost of the CGU, while the second term covers its startup/shutdown costs. The third term accounts for BESS charging costs, and the fourth term reflects the generation and motoring costs of PHES. The fifth and sixth terms represent the cost of energy procurement through DR from interruptible and shiftable loads, respectively. Equation (12) defines the regulation service cost for CGU, PHES, BESS, and DR. Equations (13) and (14) describe the opportunity costs for upward/downward reserves and penalties for load/renewable curtailment.

B. Constraints

Equation (15) regulates CGU's generation, their up/down reserve and regulation contributions, and (16) ensures that total generation and ramping remain within their technical limits.

$$\begin{aligned} P_{g,t} + \varrho^{up}_{g,t} + r^{u}_{g,t} &\leq \bar{P}_g z_{g,t}, \\ P_{g,t} - \varrho^{dn}_{g,t} - r^{d}_{g,t} &\geq \underline{\mathrm{P}}_g z_{g,t}; \forall g, t \end{aligned} \tag{15}$$

$$\begin{aligned} P_{g,t} - P_{g,t-1} + \varrho^{up}_{g,t} + r^{u}_{g,t} + r^{d}_{g,t-1} &\leq \sigma^{u}_g z_{g,t-1} + \kappa^{su}_g u_{g,t}, \\ P_{g,t-1} - P_{g,t} + \varrho^{dn}_{g,t} + r^{u}_{g,t-1} + r^{d}_{g,t} &\leq \sigma^{d}_g z_{g,t} + \kappa^{sd}_g v_{g,t}; \forall g, t \end{aligned} \tag{16}$$

Constraints (17)-(19) model PHES operations in detail. Power generation and consumption are determined by the heads of the upper and lower reservoirs (H^{ur}, H^{lr}) and water discharge quantities ($\wp^{+}h,t$, $\wp^{-}h,t$) corresponding to generating and motoring modes, respectively, as defined in (17). The constant ν represents the product of water density and gravitational acceleration. Equation (18) governs the water levels in the reservoirs, while (19) ensures that energy, regulation, and reserve schedules respect the power limits of both modes.

$$P^{gen}_{h,t} = \eta^{+}_h H^{ur} \wp^{+}_{h,t} \nu, \; P^{con}_{h,t} = (H^{ur} \wp^{-}_{h,t} \nu)/\eta^{-}_h; \forall h, t \tag{17}$$

$$\begin{aligned} \aleph^{ur}_{h,t} &= \aleph^{ur}_{h,t-1} + (\wp^{-}_{h,t} - \wp^{+}_{i,t})\Delta t, \\ \aleph^{lr}_{h,t} &= \aleph^{lr}_{h,t-1} + (\wp^{+}_{h,t} - \wp^{-}_{h,t})\Delta t; \forall h, t \end{aligned} \tag{18}$$

$$P^{+}_{h,t} + \varrho^{up}_{h,t} + r^{u}_{h,t} \leq P^{gen}_{h,t}, \; P^{-}_{h,t} + \varrho^{dn}_{h,t} + r^{d}_{h,t} \quad \leq P^{con}_{h,t}; \forall h, t \tag{19}$$

The BESS model incorporates the state of charge (SOC) and rated power as defined in (20)-(23). Constraints (20) and (21) define the charge and discharge rate thresholds, while SOC is expressed in (22). Equation (23) enforces the SOC limit and prevents simultaneous charging and discharging.

$$\underline{P}^{-}_e z^{-}_{e,t} \leq P^{-}_{e,t} + \varrho^{dn}_{e,t} + r^{d}_{e,t} \leq \bar{P}^{-}_e z^{-}_{e,t}; \forall e, t \tag{20}$$

$$\underline{P}^{+}_e z^{+}_{e,t} \leq P^{+}_{e,t} + \varrho^{up}_{e,t} + r^{u}_{e,t} \leq \bar{P}^{+}_e z^{+}_{e,t}; \forall e, t \tag{21}$$

$$\begin{aligned} \chi_{e,t} - \chi_{e,t-1} = [(P^{-}_{e,t} + \varrho^{dn}_{e,t} + r^{d}_{e,t})\eta^{-}_e \\ - \frac{(P^{+}_{e,t} + \varrho^{up}_{e,t} + r^{u}_{e,t})}{\eta^{+}_e}] \triangle t; \forall e, t \end{aligned} \tag{22}$$

$$\underline{\chi}_e \leq \chi_{e,t} \leq \bar{\chi}_e, \; z^{+}_{e,t} + z^{-}_{e,t} \leq 1; \forall e, t \tag{23}$$

Constraints (24)-(28) govern interruptible and shiftable DR. Constraint (24) ensures the energy, regulation, and reserve contributions of interruptible DR remain within defined limits. Constraint (25) imposes a maximum participation time for DR resources, with Ω as an integer. Equations (26) and (27) define the upper and lower bounds for shiftable DR participation. Equation (28) prevents simultaneous increments and decrements in DR resources, ensuring the net energy change through shiftable DR is zero.

$$\underline{\mathrm{P}}_{l,t} z_{l,t} \leq P_{l,t} + \varrho^{up}_{l,t} + r^{u}_{l,t} \leq \bar{P}_{l,t} z_{l,t}; \forall l, t \tag{24}$$

$$\sum_{t \in T} z_{l,t} \leq \Omega; \forall l \tag{25}$$

$$0 \leq P^{+}_{\grave{l},t} + \varrho^{up}_{\grave{l},t} + r^{u}_{\grave{l},t} \leq \bar{P}_{\grave{l},t} z^{+}_{\grave{l},t}; \forall \grave{l}, t \tag{26}$$

$$-\bar{P}_{\grave{l},t} z^{-}_{\grave{l},t} \leq P^{-}_{\grave{l},t} + \varrho^{dn}_{\grave{l},t} + r^{d}_{\grave{l},t} \leq 0; \forall \grave{l}, t \tag{27}$$

$$z^{+}_{\grave{l},t} + z^{-}_{\grave{l},t} \leq 1, \; \sum_{t \in T} (P^{+}_{\grave{l},t} + P^{-}_{\grave{l},t}) = 0 \tag{28}$$

Equation (29) governs the distribution of upward and downward reserves among active resources. Constraint (30) ensures the procured FRP meets the overall reliability requirements of the SO. Additionally, constraint (31) enforces the minimum admission requirements for FRP capacity and reliability. Since (30) is non-linear, a piecewise linearisation approach is used for MILP approximation, as detailed in the Appendix. Equality constraint (32) ensures power balance at each node, while equation (33) limits power flow to permissible levels.

$$\sum_{\varpi} r^{u}_{\varpi,t} \leq \bar{R}^{up}_t, \; \sum_{\varpi} r^{d}_{\varpi \varpi \neq l,t} \leq \bar{R}^{dn}_t; \forall t \tag{29}$$

$$\Phi^{rel} \leq 1 - \Pi_{\varpi}(1 - \Phi_{\varpi} z_{\varpi,t}) \tag{30}$$

$$P_{\varpi,t} \leq \underline{P}^{\varpi}, \; \Phi_{\varpi,t} \leq \underline{\Phi}^{\varpi} \tag{31}$$

$$\begin{aligned} \sum_{g \in G_b} P_{g,t} + \sum_{e \in E_b} (P^{+}_{e,t} - P^{-}_{e,t}) + \sum_{h \in H_b} (P^{+}_{h,t} - P^{-}_{h,t}) + \\ \sum_{l \in L_b} P_{l,t} + \sum_{\grave{l} \in \grave{L}_b} (P^{+}_{\grave{l},t} + P^{-}_{\grave{l},t}) + D^{curt}_{b,t} - \sum_{w \in W_b} P^{curt}_{w,t} - \\ \sum_{s \in S_b} P^{curt}_{s,t} + \sum_{\varpi,t} r^{u}_{\varpi,t} - \sum_{\varpi \varpi \neq l,t} r^{d}_{\varpi,t} - N_{b,t} = \sum_{\grave{b} \in B_b} \varphi_{b,\grave{b},t}; \forall b, t \end{aligned} \tag{32}$$

$$-\xi_{b,\grave{b}} \leq \varphi_{b,\grave{b},t} \leq \xi_{b,\grave{b}}; \forall b, t \tag{33}$$

IV. Case Study

The proposed methodology is evaluated using the Great Britain test system with a focus on 40% RES integration. Historical and day-ahead data for load, solar irradiance, and wind speed from various locations in Great Britain are sourced from [19]. The system includes a 200MW PHES with an 8h discharge duration and a 1TMC reservoir, alongside a 50MW/200MWh BESS. Interruptible and shiftable DR are assumed to provide up to 10% of the peak load at each bus [13]. The reserve reliability requirement of SOs is set at 99.99%, with reserves procured from FRPs, including BESS, PHES, DR, and CGUs, offering reserve reliability bids of 0.85, 0.8, 0.75, and 0.98, respectively [15].

A. OEL-IF: Seasonal Dataset (Spring-2019)

The Figure 1 shows the IFs obtained by the proposed model with optimum number of base learners and for various SLs. To gauge the performance of these forecasts, three deterministic (Mean absolute error (MAE), R^2-score, and Computational time (CT) and a probabilistic metric, Average coverage error (ACE) are used [18]. Also, the number of base learners in the ensemble are increased to find a optimum value and corresponding metrics are evaluated and compared with the benchmark models. However the benchmarks are performed using offline mode [8]. As shown in Table I, all the online

models require less computational time, and ACE to obtain the IFs for further use. Also, it shows that percentage of MAE (within 2.0%) and R^2-scores (97.0%), which is a very good fit [18].

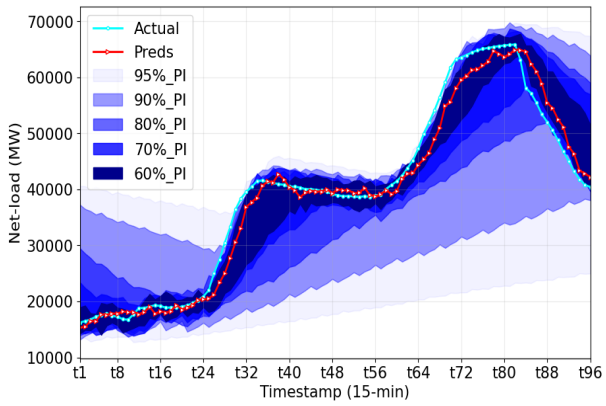

Fig. 1: Point forecasts and IFs generated for Net-load.

TABLE I: Permormance of OEL-IF models with increasing number of base learners (BL) and Benchmarks.

BL(#)/BM	MAE [MW]	R^2	CT (s)	ACE [%]
OEL-PI(2)	1707.06	0.958	128	-0.114
OEL-PI(4)	1490.32	0.968	193.5	-0.288
OEL-PI(6)	1468.99	0.969	257.6	-0.325
OEL-PI(8)	1402.12	0.973	324.6	-0.365
OEL-PI(10)	1409.20	0.973	386.44	-0.225
IPFD*	–	–	$>$ 1314.91	1.38

*Model used [8]

B. Reliability aware reserve procurement

To evaluate the impact of reliability in the market-clearing model, four cases are considered. $C1$: Deterministic net-load prediction without accounting for uncertainty, with only CGUs providing energy and reserve. $C2$: Extends $C1$ by incorporating OELIF net-load uncertainty at a 60% SL without reliability awareness (constant reserve prices). $C3$: Considers net-load uncertainty at varying SLs, without reliability awareness, while integrating multiple FRPs (DR, BESS, PHES, CGU). $C4$: Incorporating reliability aware reserve pricing in $C3$. As shown in Table II, $C1$ follows a greedy strategy since uncertainty is ignored. However, neglecting uncertainty can lead to high operational costs. In $C2$, the inclusion of net-load uncertainty at SL 60% increases costs compared to $C1$, but since only CGUs participate, reliability is the highest.

$C3$ improves cost-optimality over $C1$ and $C2$ by allowing FRP participation, but overall reliability decreases due to the inclusion of less reliable resources. Among all cases, $C4$ achieves the lowest total operating cost (TOC) and reserve cost (RC) while maintaining the highest reliability. In $C3$, the constant reserve price leads the system to prioritize procurement from the most reliable resource, i.e., CGUs, keeping costs lower. However, as the SL increases, participation from less reliable resources grows, reducing system reliability since reliability constraints are not enforced. In $C4$, reliability-aware reserve pricing ($C^r \Phi_{\varpi}$) encourages broader participation without compromising overall reliability, further reducing TOC and RC. This is further validated by Fig. 2, which compares the participation of different FRPs in $C3$ and $C4$ at an SL of 70%.

TABLE II: Impact of reliability on reserve procurement.

Cases	SL	TOC* (M$)	RC@ (M$)	Reliability (%)	Time (s)
C1	-	25.32	2.14	-	703
C2	60%	40.43	4.71	99.99	1002
C3	60%	39.42	3.55	62.1411	1162
	70%	43.19	4.93	60.2342	1190
	80%	48.36	6.82	57.3261	1206
	90%	54.37	7.86	55.6213	1294
	95%	61.09	8.36	50.3768	1361
C4	60%	35.37	3.04	99.9941	1204
	70%	39.27	4.51	99.9938	1235
	80%	45.58	5.97	99.9937	1324
	90%	52.34	6.79	99.9934	1407
	95%	58.73	7.44	99.9934	1483

*Total operating cost, @Reserve cost

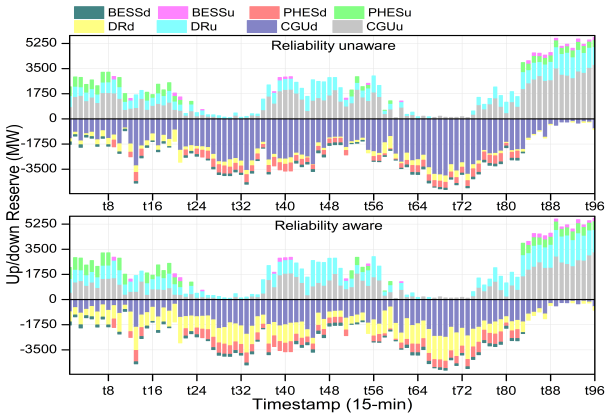

Fig. 2: Up/down reserve comparison for reliability aware and aware optimization for 70% SL.

V. Conclusion

In this work, an OELIF-based net-load uncertainty model is proposed, enabling OR quantification at different SLs. The model dynamically updates prediction intervals using real-time data streams, improving adaptability to changing system conditions. A network-constrained market-clearing framework is further developed for reliability-aware reserve procurement. Simulation results verify the effectiveness of the OELIF model in capturing net-load variations with MAE ranges between (1.99-2.43)%, and R^2-score as 97%, and ACE ranges between (-0.365 to -0.114)%. Moreover, reliability-aware reserve allocation enhances market liquidity and reduces costs (TOC by 4–10% and RC by 11–14%), while enabling the integration of less reliable resources without compromising system reliability. Future work will explore multiple reliability blocks and incorporate correlated uncertainties.

References

[1] Y. Li, C. Wan, D. Chen, and Y. Song, "Nonparametric probabilistic optimal power flow," *IEEE Trans. Power Syst.*, vol. 37, no. 4, pp. 2758–2770, 2022.

[2] Y. Xu, C. Wan, H. Liu, C. Zhao, and Y. Song, "Probabilistic forecasting-based reserve determination considering multi-temporal uncertainty of renewable energy generation," *IEEE Trans. Power Syst.*, vol. 39, no. 1, pp. 1019–1031, 2024.

[3] Y. Bapin, M. Mussard, and M. Bagheri, "Estimation of operating reserve capacity in interconnected systems with variable renewable energy using probabilistic approach," in *IEEE Int. Conf. Probab. Methods Appl. Power Syst. (PMAPS)*, 2018, pp. 1–6.
[4] Z. Meng, Y. Guo, W. Tang, and H. Sun, "Nonparametric multivariate probability density forecast in smart grids with deep learning," *IEEE Trans. Power Syst.*, vol. 38, no. 5, pp. 4900–4915, 2023.
[5] J. Wang, T. Niu, H. Lu, W. Yang, and P. Du, "A novel framework of reservoir computing for deterministic and probabilistic wind power forecasting," *IEEE Trans. Sust. Energy*, vol. 11, no. 1, pp. 337–349, 2020.
[6] Y. Shi and N. Chen, "Conditional kernel density estimation considering autocorrelation for renewable energy probabilistic modeling," *IEEE Trans. Power Syst.*, vol. 36, no. 4, pp. 2957–2965, 2021.
[7] H. Liu and C. Chen, "Data processing strategies in wind energy forecasting models and applications: A comprehensive review," *Applied Energy*, vol. 249, pp. 392–408, 2019.
[8] C. Zhao, C. Wan, and Y. Song, "Operating reserve quantification using prediction intervals of wind power: An integrated probabilistic forecasting and decision methodology," *IEEE Trans. Power Syst.*, vol. 36, no. 4, pp. 3701–3714, 2021.
[9] Zhao, Changfei and Wan, Can and Song, Yonghua, "An adaptive bilevel programming model for nonparametric prediction intervals of wind power generation," *IEEE Trans. Power Syst.*, vol. 35, no. 1, pp. 424–439, 2019.
[10] C. Wan, C. Zhao, and Y. Song, "Chance constrained extreme learning machine for nonparametric prediction intervals of wind power generation," *IEEE Trans. Power Syst.*, vol. 35, no. 5, pp. 3869–3884, 2020.
[11] M. Cao and J. Yu, "Dynamic setting method of assessment indicators for power curves of renewable energy sources considering scarcity of reserve resources," *J. Mod. Power Syst. Clean Energy*, vol. 12, no. 1, pp. 101–114, 2024.
[12] H. Li, H. Hui, and H. Zhang, "Blockchain-assisted virtual power plant framework for providing operating reserve with various distributed energy resources," *iEnergy*, vol. 2, no. 2, pp. 133–142, 2023.
[13] S. Yamujala, A. Jain, S. Sreekumar, R. Bhakar, and J. Mathur, "Enhancing power systems operational flexibility with ramp products from flexible resources," *Elect. Power Syst. Res.*, vol. 202, p. 107599, 2022.
[14] L. Herre, P. Pinson, and S. Chatzivasileiadis, "Reliability-aware probabilistic reserve procurement," *Elect. Power Syst. Res.*, vol. 212, p. 108345, 2022.
[15] N. Qi, L. Cheng, K. Huang, A. Mujeeb, F. Liu, and P. Pinson, "Reliability-aware probabilistic reserve procurement under decision-dependent uncertainty," in *IEEE Power & Energy Society General Meeting (PESGM)*. IEEE, 2024, pp. 1–5.
[16] R. Fernández-Blanco, J. M. Arroyo, and N. Alguacil, "On the solution of revenue- and network-constrained day-ahead market clearing under marginal pricing—part i: An exact bilevel programming approach," *IEEE Trans. Power Syst.*, vol. 32, no. 1, pp. 208–219, 2017.
[17] R. S. Sutton, "Two problems with backpropagation and other steepest-descent learning procedures for networks," pp. 823–831, 1986.
[18] A. K. Nayak, K. C. Sharma, R. Bhakar, and H. Tiwari, "Probabilistic online learning framework for short-term wind power forecasting using ensemble bagging regression model," *Energy Conversion and Management*, vol. 323, p. 119142, 2025.
[19] "Modern-era retrospective analysis for research and application," 2024, [Online]. Available: http://www.soda-pro.com/web-services/meteo-data/merra. (Accessed Apr. 2024).

APPENDIX
PIECEWISE LINEARISATION OF RELIABILITY EQUATION

The use of logarithmic law $ln(\Pi_{\varpi} f_{\varpi}) = \sum_{\varpi} ln(f_{\varpi})$ allows to reformulate (30) as

$$ln(1-\Phi^{rel}) \geq \sum_{\varpi} ln(1-\Phi_{\varpi} z_{\varpi,t}) \tag{34}$$

A piecewise function is now employed to approximate the logarithmic equation in (34). Furthermore, it should be noted that for $\Phi_{\varpi} \in [0,1]$ and $z_{\varpi,t} \in \{0,1\}$ it holds that

$$\sum_{\varpi} ln(1-\Phi_{\varpi} z_{\varpi,t}) = \sum_{\varpi} z_{\varpi,t} ln(1-\Phi_{\varpi}) \tag{35}$$

Therefore, the non-linear terms in the inequality constraint (30) are: $ln(\Pi_{\varpi} f_{\varpi})$ and $ln(1-\Phi_{\varpi})$, which need to be approximated using piecewise linearisation.

Piecewise linear approximation for $ln(1-\Phi)$: Divide the range of Φ into Y intervals $[a_y, a_{y+1}]$ where a_y and a_{y+1} are the endpoints of the y-th interval. For each interval, approximate $ln(1-\Phi)$ linearly as:

$$\begin{gathered} ln(1-\Phi) \approx (u_y \Phi + v_y), \text{for } a_y \leq \Phi \leq a_{y+1}; \\ u_y = \frac{ln(1-a_{y+1}) - ln(1-a_y)}{a_{y+1}-a_y}, v_y = ln(1-a_y) - u_y a_y \end{gathered} \tag{36}$$

Introduce binary variables δ_y, ensuring that only one interval is active.

$$a_y \delta_y \leq \Phi \leq a_{y+1} \delta_y, \text{ and } \sum_y \delta_y = 1 \tag{37}$$

The equation (30) is now fully linearized as (38) along with the additional constraints given in equation (39):

$$\sum_y (u_y \Phi^{rel} + v_y) \delta_y^{rel} \geq \sum_{\varpi} z_{\varpi,t} \sum_y (u_y \Phi_{\varpi} + v_y) \delta_y^{\varpi} \tag{38}$$

$$\begin{gathered} a_y \delta_y^{rel} \leq \Phi^{rel} \leq a_{y+1} \delta_y^{rel}, \text{ and } \sum_y \delta_y^{rel} = 1 \\ a_y \delta_y^{\varpi} \leq \Phi_{\varpi} \leq a_{y+1} \delta_y^{\varpi}, \text{ and } \sum_y \delta_y^{\varpi} = 1 \end{gathered} \tag{39}$$